INTL JOURNAL OF ELECTRONICS AND TELECOMMUNICATIONS, 2023, VOL. 69, NO. 4, PP. 775-784
Manuscript received February 20, 2023; revised October, 2023. DOI: 10.24425/ijet.2023.147701

QIBMRMN: Design of a Q-Learning based Iterative sleep-scheduling & hybrid Bioinspired Multipath Routing model for Multimedia Networks

Minaxi Doorwar, and P Malathi

Abstract*—Multimedia networks utilize low-power scalar nodes to modify wakeup cycles of high-performance multimedia nodes, which assists in optimizing the power-to-performance ratios. A wide variety of machine learning models are proposed by researchers to perform this task, and most of them are either highly complex, or showcase low-levels of efficiency when applied to large-scale networks. To overcome these issues, this text proposes design of a Q-learning based iterative sleep-scheduling and fuses these schedules with an efficient hybrid bioinspired multipath routing model for large-scale multimedia network sets. The proposed model initially uses an iterative Q-Learning technique that analyzes energy consumption patterns of nodes, and incrementally modifies their sleep schedules. These sleep schedules are used by scalar nodes to efficiently wakeup multimedia nodes during adhoc communication requests. These communication requests are processed by a combination of Grey Wolf Optimizer (GWO) & Genetic Algorithm (GA) models, which assist in the identification of optimal paths. These paths are estimated via combined analysis of temporal throughput & packet delivery performance, with node-to-node distance & residual energy metrics. The GWO Model uses instantaneous node & network parameters, while the GA Model analyzes temporal metrics in order to identify optimal routing paths. Both these path sets are fused together via the Q-Learning mechanism, which assists in Iterative Adhoc Path Correction (IAPC), thereby improving the energy efficiency, while reducing communication delay via multipath analysis. Due to a fusion of these models, the proposed Q-Learning based Iterative sleep-scheduling & hybrid Bioinspired Multipath Routing model for Multimedia Networks (QIBMRMN) is able to reduce communication delay by 2.6%, reduce energy consumed during these communications by 14.0%, while improving throughput by 19.6% & packet delivery performance by 8.3% when compared with standard multimedia routing techniques.

***Keywords*—multimedia; network; Q-Learning; GWO; GA; Adhoc; QoS; iterative; process**

I. INTRODUCTION

THE provision of services reliant on the connectivity of numerous intelligent devices, sensors, actuators, and the like is expected to have a substantial impact on people's everyday life (IoT). According to some projections, there will be more Internet-connected gadgets on the planet in 2021 than there are people. When completely implemented, the Internet of Things will allow a profusion of cutting-edge services, such as those pertaining to rich media streaming with Low-Energy-First Electoral Multipath Alternating Multihop Routing (LEMH) [1, 2], intelligent surveillance [3, 4], smart home applications with Cross Layer Optimizations [5, 6], etc. Wireless sensor networks (WSN) and more recently wireless multimedia sensor networks are essential for IoT applications to operate(WMSN). Figure 1 illustrates how multimedia sensor nodes (MSNs) are often scattered around an area to collect environmental data and send it to distant servers for analysis. After then, anybody who is interested may see or hear it. Multimedia techniques such as video conferencing, VoD, and real-time material dissemination are presently the most common ways of communication. According to research in [7, 8, 9, 10], traffic from Multipath Routing will be highly effective for real-time use cases like satellite communications.Video surveillance becoming a more crucial use for WMSNs, it is anticipated that in comparison to [11, 12, 13, 14], Internet traffic would grow by a factor of seven. We'll put this growth into action between 2017 and 2025. Before WMSN applications may be effectively deployed and function at their best, a few significant issues must be resolved. To begin, incorporating multimedia components into IoT systems [15, 16, 17, 18] is challenging as it entails redesigning present functionalities and adding new ones. More bandwidth is used for the transmission of multimedia via WSNs than for the exchange of straightforward data. WMSN traffic also includes burst mode and other time-sensitive delivery restrictions. The second issue is that multimedia sensing devices have limited memory, computing capacity, and, most significantly, energy resources. Even if the data contains multimedia, which often requires speedy transmission and robust processing, this still holds true.

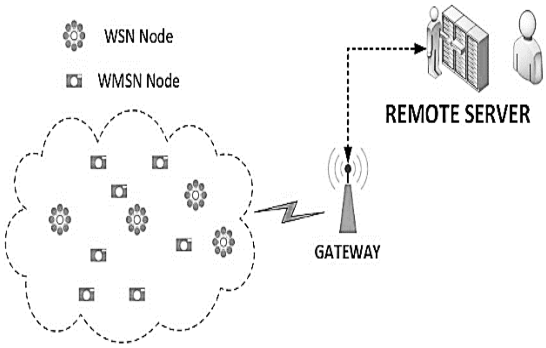

Fig. 1. A typical use case for Wireless Multimedia Sensor Node communications

Authors are with SPPU, E&TC Department, India (e-mail: minaxi.rawat@gnail.com, pjmalathi@dypcoeakurdi.ac.in).

Additionally, WMSN nodes with battery packs may sometimes function for very extended periods of time without the assistance of a human operator. Therefore, WMSN users and operators must give equal weight to two objectives: lowering energy consumption and increasing customer awareness of service quality. The difficulty of guaranteeing that the underlying applications have the required lifespan, throughput, latency, and dependability is also overcome by the WMSN network architecture. For instance, the sensor nodes used in these systems may be configured to indicate any anomalies while a target is being followed or watched. The quality of the video stream, which is the most crucial factor in this case, has a significant influence on the throughput requirements of the system and improves via Multipath Genetic Algorithm (MGA) [19, 20]. Applications that prioritize energy conservation include those that depend on sensor nodes to routinely monitor and send data. The development and operation of WMSN in a way that it satisfies the requirements of the diverse range of potential applications may be difficult. Parameter tuning, which involves modifying different network parameters to suit the requirements of the application, is one efficient way to address these problems. Although these techniques have many advantages [21, 22, 23, 24], they also have some serious drawbacks. Making modifications to the network's settings is challenging and time-consuming due to the unpredictable nature of the WMSN environment. However, the tuning parameters that are frequently generated are poor. If a sensor node is highly adjustable, has several parameters, and has a wide range of possible values for each parameter, finding the best settings for it could be difficult. Finding the ideal settings to use has become more challenging due to the dynamic volatility of the sensor node's surroundings. The use of dynamic optimization-based approaches [25, 26, 27, 28, 29, 30] may be put to use in making decisions about the best network parameters so that sensor networks may adapt their operations to the needs of the application and the environment. Due to the high level of environmental unpredictability, these methods guarantee that sensor networks operate well and that the sensor nodes within them retain their functioning. The Vehicular Ad-Hoc Reliable Routing (VARR) [31, 32, 33, 34] is a dynamic optimization method that should be taken into account for WMSNs. This is due to the fact that in a highly dynamic environment where variables like wireless channel conditions, traffic, and energy restrictions are always changing, effective decision-making is crucial. With WMSNs, the Software Defined Networks (SDN) [35, 36, 37, 38] is a dynamic optimization approach that is effective. Node radio transmission often uses the bulk of the network's power in a WMSN [39]. The Medium Access Control (MAC) layer controls radio network access in wireless communications. It is essential to prioritize the MAC layer's energy efficiency in order to provide the longest potential lifetime for WMSNs. Although there are several ways to regulate radio transmission, duty cycle management is one of the most effective. Duty cycle techniques include intermittently stopping the radio transmission of sensor nodes as a way to save power. Duty cycle techniques are widely used in WSNs, particularly in the two main operating systems Tiny OS and Contiki1, which were created specifically for WSNs with BigNum Network Coding (BNNC) [40] These operating systems are among the greenest options on the market right now. Under a Duty Cycle method, the QoS may deteriorate dramatically in terms of latency and throughput. [8] We must treat this issue seriously. For the purpose of energy-aware data transmission over WMSNs, several research methodologies [41] have been put forth to improve QoS performance when Duty Cycle approaches are implemented at the MAC layer. Part II goes into more depth about the numerous focuses and methods employed to produce these solutions. A thorough analysis of the numerous varieties of applications and associated traffic is one of the most crucial steps in designing any solution. For a specific application, data like temperature readings, node locations, and multimedia files can all be sent simultaneously in a stream format. It can be difficult to give systems that process a wide range of traffic types and associated requirements adequate support. Multimedia content distribution when combined with high-rate data transmission in real time creates a significant barrier for heterogeneous deployments.

Thus, it can be observed that a wide variety of machine learning models are proposed by researchers to perform this task, and most of them are either highly complex, or showcase low-levels of efficiency when applied to large-scale networks. To overcome these issues, next section of this text proposes design of a Q-learning based iterative sleep-scheduling and fuses these schedules with an efficient hybrid bioinspired multipath routing model for large-scale multimedia network sets. The proposed model was evaluated on large-scale network scenarios in section 3, where its performance was estimated & compared in terms of communication delay, energy efficiency, packet delivery performance and throughput levels w.r.t. existing multimedia network models. Finally, this text is concluded with some interesting observations about the proposed model, and also recommends methods to further improve its performance under different scenarios.

II. DESIGN OF THE PROPOSED Q-LEARNING BASED ITERATIVE SLEEP-SCHEDULING & HYBRID BIOINSPIRED MULTIPATH ROUTING MODEL FOR MULTIMEDIA NETWORKS

The review of existing multipath routing models for multimedia networks reveals that researchers have proposed a wide variety of machine learning models to perform this task, the majority of which are either highly complex or inefficient when applied to large-scale networks. This section discusses the design of a Q-learning based iterative sleep-scheduling and fuses these schedules with an efficient hybrid bioinspired multipath routing model for large-scale multimedia network sets in order to address these issues. Design of the model is depicted in figure 2, where it can be observed that the proposed model employs an iterative Q-Learning technique that analyzes the energy consumption patterns of nodes and modifies their sleep schedules incrementally. Scalar nodes use these sleep schedules to efficiently awaken multimedia nodes during ad hoc communication requests. These communication requests are handled by a combination of Grey Wolf Optimizer (GWO) and Genetic Algorithm (GA) models, which aid in the determination of optimal paths. These paths are estimated by analysing temporal throughput and packet delivery performance in conjunction with node-to-node distance and residual energy metrics. The GWO Model uses instantaneous node and network parameters to identify optimal routing paths, whereas the GA Model analyzes temporal metrics. These two path sets are merged using the Q-Learning mechanism, which aids in Iterative Adhoc Path Correction (IAPC), thereby enhancing energy efficiency and minimizing communication delay via multipath analysis.

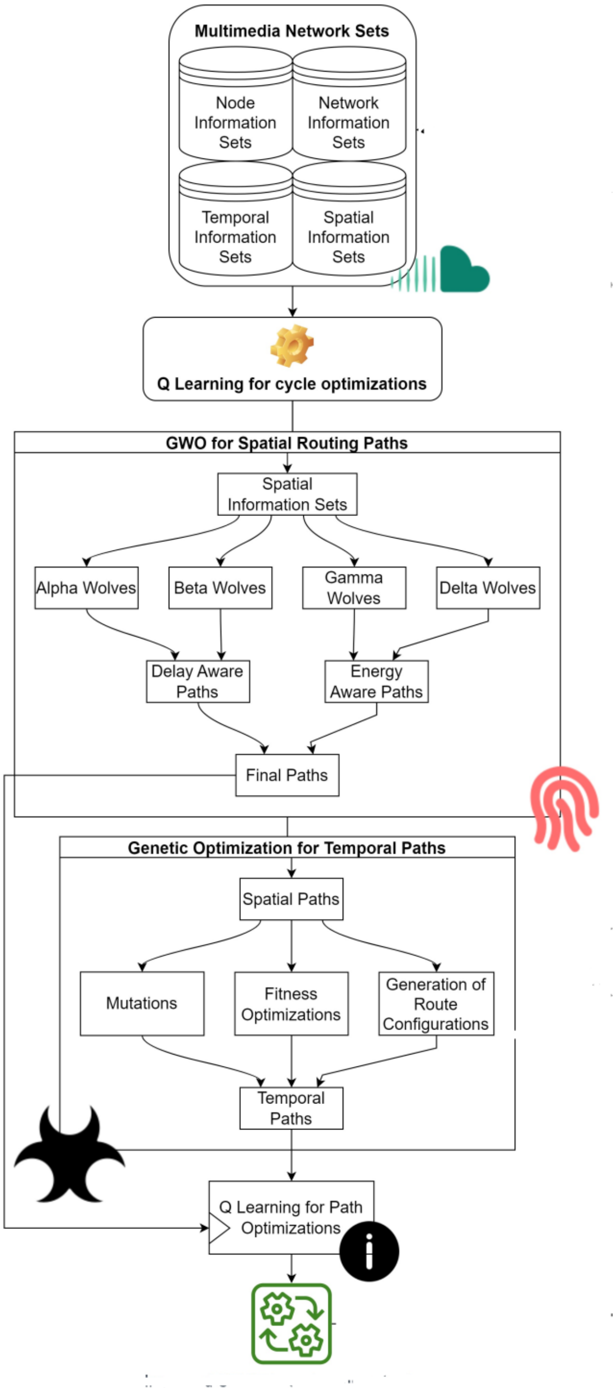

Fig. 2. Design of the proposed dual bioinspired model with Q Learning for iterative optimizations of routing process

To perform these tasks, the model initially collects large scale data sets that consist of node locations, energy levels, temporal throughput, temporal packet delivery ratio (PDR), link quality, network bandwidth, and other parameter sets. The collected information sets are given to a Q-Learning based model, which initially estimates a Q-Level for every node via equation 1,

$$Q = \sum_{i=1}^{N_c} \frac{PDR_i}{100} + \frac{THR_i}{Max(THR_i)} + \frac{Max(E)}{E_i} \quad (1)$$

Where, N_c represents total number of temporal communications for each of the nodes, while PDR, THR & E represents their temporal PDR, throughput and energy consumption levels. Based on these Q values, a correlative mapping is done between scalar and multimedia nodes. To perform this mapping, a correlative Q-Level (QC) is estimated for each scalar node-to-multimedia node pair via equation 2,

$$QC_{i,j} = \frac{Q_i}{d_{i,j}} \quad (2)$$

Where, $d_{i,j}$ represents distance between the multimedia and scalar nodes. The QC vector is sorted in descending order, and nodes are mapped starting from top of this sorted vector, thereby assisting in selection of node pairs with minimum distance and maximum temporal performance levels. The duty cycles of these node pairs are used in order to update duty cycle of the multimedia node via equation 3,

$$D_i(New) = D_i(Old) + \frac{Q_i}{QC_{i,j}} * (Q_i - Q_j) + \frac{Q_i + Q_j}{QC_{i,j}} * Max(Q) - D_j \quad (3)$$

Where, D represents duty cycle of individual nodes. Based on this updated cycle value, multimedia nodes are put to sleep, while scalar nodes are mostly in wakeup phase, waiting for new packet requests. These packet requests are initially processed by a Grey Wolf Optimization (GWO) Model, which works as per the following process,

- To initialize the optimizer, setup the following constants,
  - Total iterations for which the GWO will reconfigure its Wolves (N_i)
  - Total Wolves that will take part in the optimization process (N_w)
  - Individual social learning rates the Wolves (L_r)
  - Source (src) and Destination ($dest$) node IPs
- Initially, generate N_w Wolves via the following process,
  - Stochastically select a 1-hop neighbour for current source node via equation 4,

$$N_{sel} = STOCH(1, N_{1hop}), where\ d_{sel,src} < d_{ref}\ \&\ d_{sel,dest} < d_{ref} \quad (4)$$

Where, $STOCH$ represents a Markovian process used for generation of stochastic numbers, while $d_{i,j}$ represents Euclidean distance between the i & j nodes, N_{1hop} are the 1-hop neighbours of current source node, and d_{ref} is the reference distance between source & destination node pairs.

  - Repeat this process for all nodes till destination node is reached, and then estimate Spatial Wolf fitness via equation 5,

$$f_{sw} = \sum_{i=0\,(src)}^{N_{path}-1} \frac{d_{i,i+1}}{E_i * N_{path}} \quad (5)$$

Where, N_{path} represents number of nodes present in the current path sets.

- Once all Wolves are generated, then a Wolf level fitness threshold is estimated via equation 6,

$$f_{th} = \sum_{i=1}^{N_W} f_{sw_i} * \frac{L_{r_i}}{N_W} \quad (6)$$

- Initially all L_w are equated to a constant, and are later modified via Wolf Marking operations, that works as per the following process,

Mark the Wolf as 'Alpha', if $f_{sw} > 2 * f_{th}$ (7)

Else,

Mark the Wolf as 'Beta', if $f_{sw} > f_{th}$ (8),

and change its learning rate via equation 11,

$$L_r(New) = L_r(Old) + \sum_{i=1}^{N(Alpha)} \frac{L_r}{N(Alpha)} \quad (9)$$

Where, $N(Alpha)$ represents the Alpha Wolf particles.

Mark the Wolf as 'Gamma', if $f_{sw} > L_w * f_{th}$ (10),

and change its learning rate via equation 11,

$$L_r(New) = L_r(Old) + \sum_{i=1}^{N(Beta)} \frac{L_r}{N(Beta)} \quad (11)$$

Where, $N(Beta)$ represents the Beta Wolf particles.

- Otherwise, Mark the Wolf as 'Delta', and change its learning rate via equation 12,

$$L_r(New) = L_r(Old) + \sum_{i=1}^{N(Gamma)} \frac{L_r}{N(Gamma)} \quad (12)$$

Where, $N(Gamma)$ represents the Gamma Wolf particles.

- This process is repeated for N_i iterations, and Wolf fitness & learning rates are modified for continuous iterative optimizations.

All the Wolves Marked as 'Alpha' Wolves are reiterated via Genetic Algorithm (GA), which assists in incorporating temporal performance metrics into the selected routes. This GA Model works as per the following process,

- Setup the Number of Solutions for GA via equation 13,

$$N_s = N(Alpha) \quad (13)$$

- Setup the learning rate of GA via equation 14,

$$L_r = \sum_{i=1}^{N(Alpha)} \frac{L_{r_i}}{N(Alpha)} \quad (14)$$

- Now, scan through each of the solutions for N_i iterations, and perform the following operations,
  - For each solution, estimate its temporal fitness via equation 15,

$$f = \frac{1}{N_{path} * N_c} \sum_{i=1}^{N_{path}} \sum_{j=1}^{N_c} \frac{D_{i,j}}{Max(D)} + \frac{E_{i,j}}{Max(E)} + \frac{100}{PDR_{i,j}} + \frac{Max(THR)}{THR_{i,j}} \quad (15)$$

Where, D, E, PDR & THR represents the temporal delay levels, temporal energy levels, temporal PDR levels, and temporal throughput levels for each of the N_c communications.

  - Once these values are estimated for all solutions, then identify fitness threshold via equation 16,

$$f_{th} = \sum_{i=1}^{N_s} f_i * \frac{L_r}{N_s} \quad (16)$$

  - For all solutions with $f \geq f_{th}$, modify their configurations via the following process,
    - Stochastically select a solution with $f < f_{th}$
    - Replace a in-path node from this solution with the in-path node of the solution that is being modified, as per equation 17,

$$N(New) = STOCH\left(N_{1hop}(Current)\right) \quad (17)$$

Where, $N(New)$ represents the new node for solution that is being modified, while $N_{1hop}(Current)$ is the solution that is elected for replacement of nodes.

    - Based on this process, evaluate solution fitness via equation 17, and update route configurations.
- This process is repeated for N_i iterations, which assists in identification of solution sets with minimum fitness levels.

Once all iterations are completed, then select the solution with minimum fitness levels, and use it for routing operations. After completion of one routing operation, the fitness threshold of GA is updated via equation 18,

$$L_r(New) = L_r(Old) + \frac{Min(f)}{Max(f)} * \left(Max(f) - Min(f)\right) + \frac{Min(f)}{Min(f) + Max(f)} * Max(f) \quad (18)$$

This Q-Learning based update assists in incrementally optimizing the learning rate, which improves node selection efficiency during the routing process. This efficiency is evaluated in terms of different routing parameters and compared with existing models in the next section of this text.

III. PERFORMANCE COMPARISON AND EVALUATION

The proposed model uses a combination of Q-Learning with Grey Wolf Optimizer (GWO) & Genetic Algorithm (GA) in order to identify optimal routes with sleep scheduling for multimedia network scenarios. The Q-Learning model enables optimization of duty cycles for scalar & multimedia nodes. These updated duty cycles are used by Grey Wolf Optimizer in order to identify spatially optimized routes, which are temporally optimized by the Genetic Algorithm based route selection process. The route optimization process is further tuned by a Q-Leaning-based operation, which assists in iterative updation of learning rates for future routing requests. In order to validate performance of this model, it is evaluated in terms of communication delay (D), energy needed during communications (E), packet delivery ratio (PDR), and throughput (T) for different communication requests. This performance is evaluated on Network Simulator (NS2), with the following network configurations as depicted in table I,

TABLE I
CONFIGURATIONS USED DURING SIMULATIONS

Network Simulation Parameter	Configuration Value Set
Propagation of nodes	Using 2 Ray Ground
Protocol for MAC operations	802.11
Queue used for interfaces	Queue with priority & drop tailing operations
Model used for Antennas	Omnidirectional
Total Multimedia Nodes	100 to 1000
Total Scalar Nodes	100 to 5000
Routing done via base protocol	AOMDV Wireless
Total dimensions of the network	1km x 1km
Energy Model	M – Multimedia, S – Scalar
Energy consumed while in idle mode	2 mW (M), 0.1 mW (S)
Energy consumed while in reception mode	3 mW (M), 0.2 mW (S)
Energy consumed while in transmission mode	5 mW (M), 1 mW (S)
Energy consumed while in sleep mode	0.0001 mW (Both)
Energy consumed while in transitioning between modes	0.01 mW (Both)
Delay needed for these transitions	0.005 s (Both)
Total energy levels of nodes during network initializations	2000 mW (M) 500 mW (S)

Using these network and node configurations, the number of node-to-node communications between were varied between linearly 100 to 1000; and same nodes were selected for routing across each route selection process. Average QoS values for energy consumption (E) was estimated via equation 19, end-to-end communication delay (D) was estimated via equation 20, packet delivery ratio (PDR) was estimated via equation 21, throughput (T) was estimated via equation 22 and delay jitter (JD) was estimated via equation 23 and evaluated for different Number of Network Communications (NNC),

$$E = \frac{1}{NNC}\sum_{i=1}^{NNC} E_{complete} - E_{initial} \quad (19)$$

Where, $E_{complete}$ & $E_{initial}$ represents the completion & initial energy of nodes during the communication operations.

$$D = \frac{1}{NNC}\sum_{i=1}^{NNC} T_{initial} - T_{complete} \quad (20)$$

Where, $T_{complete}$ & $T_{initial}$ represents the completion & initial timestamps during the communication operations.

$$PDR = \frac{1}{NNC}\sum_{i=1}^{NNC} \frac{P_{rx}}{P_{tx}} \quad (21)$$

Where, P_{rx} & P_{tx} represents the reception & transmission energy levels of nodes during these communications.

$$THR = \frac{1}{NNC}\sum_{j=1}^{NNC} \frac{P_{rx}}{D_j} \quad (22)$$

$$J = \frac{1}{NNC}\sum_{i=1}^{NNC} D_i - Mean(D) \quad (23)$$

Based on these evaluations, the average delay for different communications with 1000 Scalar & 500 Multimedia Nodes were compared with LEMH [2], MGA [19], & BNNC [40], and can be observed from table II as follows,

TABLE II
AVERAGE COMMUNICATION DELAY NEEDED DURING ROUTING FOR DIFFERENT SCENARIOS

NNC	D (ms) LEMH [2]	D (ms) MGA [19]	D (ms) BNNC [40]	D (ms) QIBMRMN
100	1.05	1.20	1.34	0.99
120	1.13	1.32	1.48	1.10
140	1.26	1.50	1.68	1.26
160	1.45	1.74	1.96	1.47
180	1.70	2.05	2.31	1.73
200	2.01	2.41	2.71	2.02
250	2.36	2.80	3.12	2.32
300	2.70	3.18	3.55	2.64
400	3.05	3.59	4.00	2.95
450	3.38	3.98	4.43	3.25
500	3.66	4.34	4.83	3.53
550	3.92	4.69	5.21	3.78
600	4.14	4.97	5.52	4.00
700	4.36	5.24	5.83	4.22
800	4.59	5.52	6.14	4.45
1000	4.84	5.82	6.47	4.69

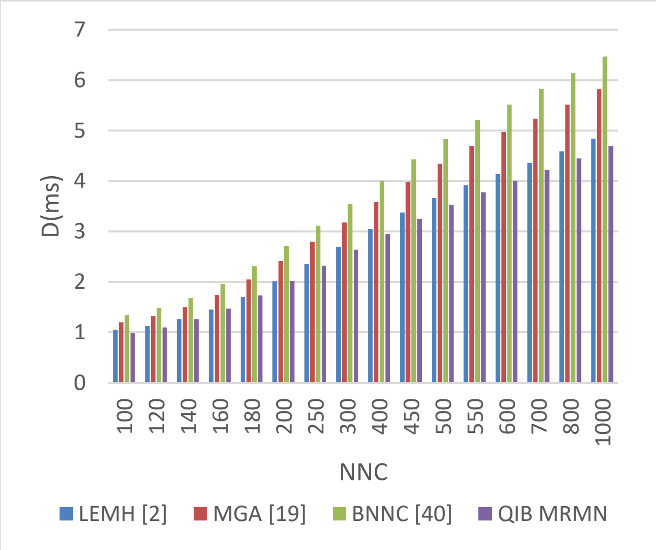

Fig. 3. Average communication delay needed during routing for different scenarios

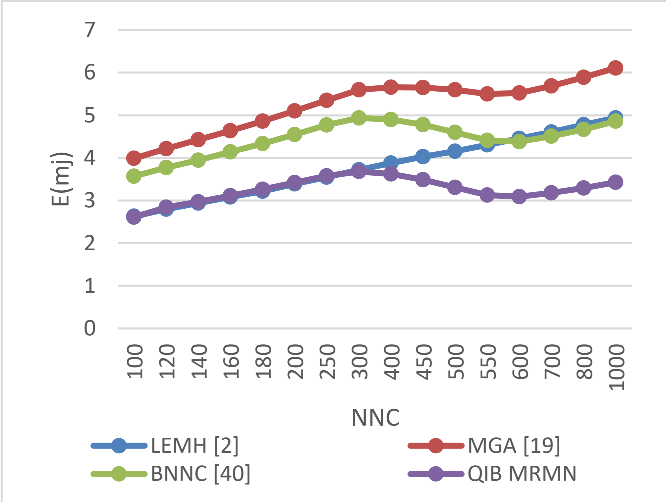

Fig. 4. Average communication energy needed during routing for different scenarios

Based on this evaluation and figure 3, it can be observed that the proposed model is capable of reducing the communication delay by 2.6% when compared with LEMH [2], 18.3% when compared with MGA [19], and 26.7% when compared with BNNC [40] under different simulation conditions. The reason for this reduction in delay is use of sleep scheduling along with distance measures in GWO & temporal delay levels in GA, which assists in selection of optimal routing paths. Similarly, the energy consumed during these communications can be observed from table III as follows,

TABLE III
AVERAGE COMMUNICATION ENERGY NEEDED DURING ROUTING FOR DIFFERENT SCENARIOS

NNC	E (mJ) LEMH [2]	E (mJ) MGA [19]	E (mJ) BNNC [40]	E (mJ) QIBMRMN
100	2.63	3.99	3.57	2.61
120	2.80	4.22	3.77	2.84
140	2.94	4.43	3.95	2.97
160	3.08	4.64	4.14	3.11
180	3.22	4.86	4.34	3.26
200	3.39	5.10	4.55	3.42
250	3.55	5.35	4.77	3.58
300	3.72	5.60	4.94	3.68
400	3.88	5.66	4.90	3.62
450	4.03	5.65	4.78	3.49
500	4.16	5.60	4.60	3.31
550	4.31	5.50	4.41	3.13
600	4.46	5.52	4.38	3.09
700	4.61	5.69	4.51	3.18
800	4.78	5.89	4.67	3.29
1000	4.94	6.11	4.86	3.43

Based on this evaluation and figure 4, it can be observed that the proposed model is capable of reducing the energy consumed during communication by 14.03% when compared with LEMH [2], 37.94% when compared with MGA [19], and 26.89% when compared with BNNC [40] under different simulation conditions. The reason for this reduction in energy is use of sleep scheduling along with use of energy levels in GWO & temporal energy levels in GA, which assists in selection of lifetime aware routing paths. Similarly, the communication throughput achieved during these communications can be observed from table IV as follows,

TABLE IV
AVERAGE COMMUNICATION THROUGHPUT ACHIEVED DURING ROUTING FOR DIFFERENT SCENARIOS

NNC	T (kbps) LEMH [2]	T (kbps) MGA [19]	T (kbps) BNNC [40]	T (kbps) QIBMRMN
100	294.55	276.53	373.58	476.02
120	297.07	278.86	376.72	480.02
140	299.52	281.19	379.90	484.06
160	302.07	283.56	383.13	488.14
180	304.62	285.92	386.34	492.19
200	307.14	288.27	389.52	496.22
250	309.66	290.62	392.69	500.26
300	312.18	292.98	395.86	504.29
400	314.69	295.35	399.03	503.71
450	317.21	297.71	402.19	501.98
500	319.73	300.06	405.35	498.99
550	322.25	302.40	408.50	494.63
600	324.77	304.73	411.65	493.42
700	327.28	307.07	414.82	495.76
800	329.80	309.42	417.99	498.75
1000	332.31	311.77	421.17	502.49

Based on this evaluation and figure 5, it can be observed that the proposed model is capable of improving the throughput achieved during communication by 36.60% when compared with LEMH [2], 40.50% when compared with MGA [19], and 19.62% when compared with BNNC [40] under different simulation conditions. The reason for this improvement in throughput is use of temporal throughput levels in GA, which assists in selection of throughput aware routing paths. This makes the model useful for high date rate applications.

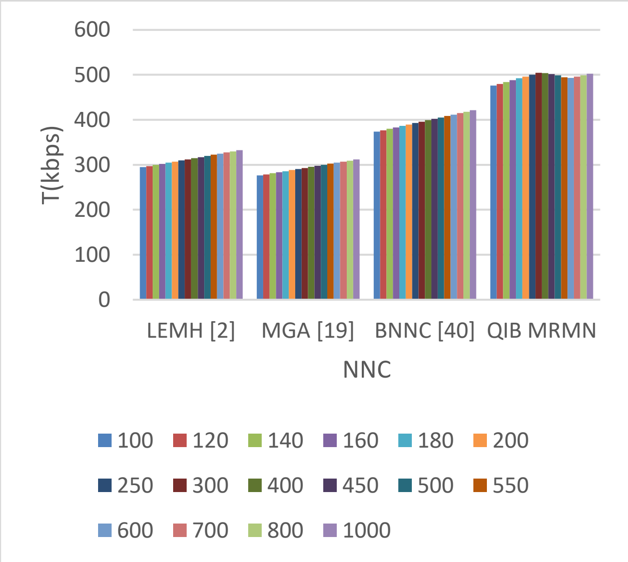

Fig. 5. Average communication throughput achieved during routing for different scenarios

Similarly, the PDR achieved during these communications can be observed from table V as follows.

TABLE V
AVERAGE PDR ACHIEVED DURING ROUTING FOR DIFFERENT SCENARIOS

NNC	PDR (%) LEMH [2]	PDR (%) MGA [19]	PDR (%) BNNC [40]	PDR (%) QIBMRMN
100	81.75	81.38	82.30	89.28
120	82.44	82.06	82.99	90.03
140	83.12	82.75	83.69	90.79
160	83.83	83.45	84.39	91.55
180	84.54	84.15	85.10	92.31
200	85.24	84.84	85.80	93.07
250	85.94	85.53	86.49	93.83
300	86.63	86.22	87.20	94.59
400	87.33	86.92	87.89	95.34
450	88.03	87.61	88.59	96.10
500	88.73	88.30	89.29	96.86
550	89.43	88.99	89.98	97.61
600	90.13	89.67	90.68	98.37
700	90.83	90.36	91.37	99.12
800	91.53	91.05	92.07	99.88
1000	92.22	91.74	92.77	99.95

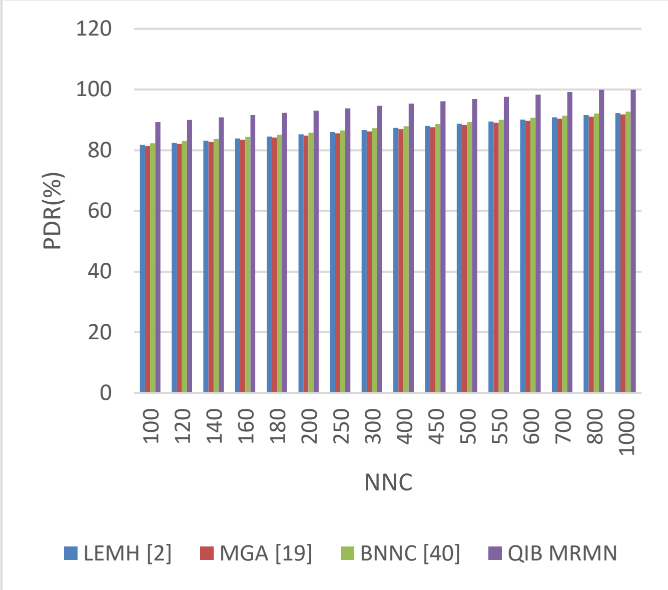

Fig. 6. Average PDR achieved during routing for different scenarios

Based on this evaluation and figure 6, it can be observed that the proposed model is capable of improving the PDR achieved during communication by 8.3% when compared with LEMH [2], 8.8% when compared with MGA [19], and 7.7% when compared with BNNC [40] under different simulation conditions. The reason for this improvement in PDR is use of temporal PDR levels in GA, which assists in selection of PDR aware routing paths. This makes the model useful for high date dissemination rate applications. Similarly, the delay jitter during these communications can be observed from table VI as follows.

TABLE VI
AVERAGE DELAY JITTER DURING ROUTING FOR DIFFERENT SCENARIOS

NNC	J (ms) LEMH [2]	J (ms) MGA [19]	J (ms) BNNC [40]	J (ms) QIBMRMN
100	1.08	1.21	1.34	0.98
120	1.16	1.33	1.48	1.09
140	1.29	1.51	1.68	1.24
160	1.48	1.76	1.96	1.45
180	1.74	2.08	2.31	1.71
200	2.06	2.44	2.71	2.00
250	2.41	2.83	3.12	2.30
300	2.77	3.22	3.55	2.60
400	3.13	3.63	4.00	2.92
450	3.46	4.03	4.43	3.21
500	3.75	4.40	4.83	3.49
550	4.01	4.74	5.21	3.74
600	4.24	5.03	5.52	3.95
700	4.47	5.31	5.83	4.17
800	4.70	5.59	6.14	4.39
1000	4.96	5.89	6.47	4.63

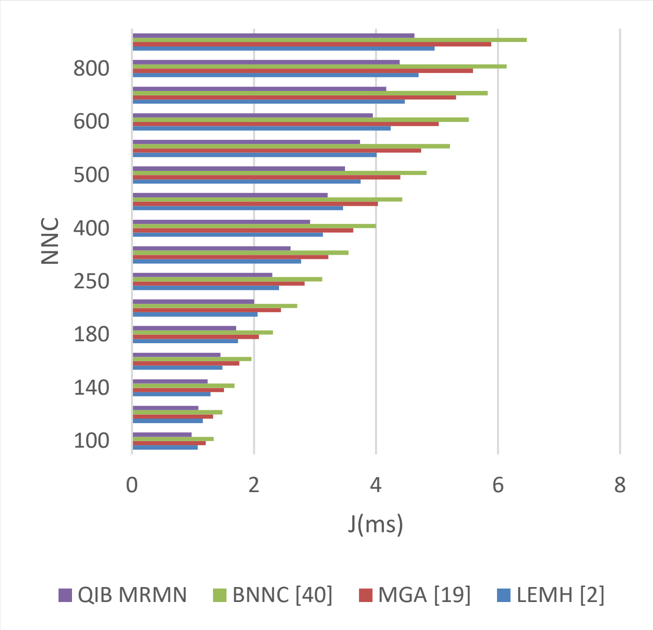

Fig. 7. Average delay jitter during routing for different scenarios

Based on this evaluation and figure 7, it can be observed that the proposed model is capable of reducing the jitter of communication by 6.08% when compared with LEMH [2], 20.23% when compared with MGA [19], and 27.58% when compared with BNNC [40] under different simulation conditions. The reason for this reduction is use of temporal delay & throughput levels in GA, which assists in selection of low jitter routing paths. This makes the model useful for applications that need high data consistency during communications. Due to these optimizations, the proposed model is useful for a wide variety of deployments that require low delay, low energy consumption, high throughput, high PDR and low communication jitter, under real-time scenarios.

IV. Conclusion and Future Scope

Combining Q-Learning with Grey Wolf Optimizer (GWO) and Genetic Algorithm (GA), the proposed model QIBMRMN identifies optimal routes with sleep scheduling for multimedia network scenarios. The Q-Learning model enables duty cycle optimization for scalar and multimedia nodes. Grey Wolf Optimizer uses these updated duty cycles to identify spatially optimized routes, which are temporally optimized by a Genetic Algorithm-based route selection procedure. A Q-Learning-based operation is used to fine-tune the route optimization process by assisting with the iterative increase of learning rates for future routing requests. On the basis of delay evaluation, the proposed model is capable of reducing communication delay by 2.6% compared to LEMH [2], 18.3% compared to MGA [19], and 26.6% compared to BNNC [40] under various simulation conditions. This reduction in delay is due to the utilization of sleep scheduling in conjunction with distance measurements in GWO and temporal delay levels in GA, which aids in the selection of optimal routing paths. On the basis of energy evaluation, it can be seen that the proposed model is capable of reducing the energy consumed during communication by 14.03% compared to LEMH [2], 37.94% compared to MGA [19], and 26.89% compared to BNNC [40] under various simulation conditions. This decrease in energy is due to the use of sleep scheduling in conjunction with the utilization of energy levels in GWO and temporal energy levels in GA, which aids in the selection of lifetime-aware routing paths. On the basis of throughput evaluation, it can be seen that the proposed model is capable of increasing communication throughput by 36.60% when compared to LEMH [2], 40.5% when compared to MGA [19], and 19.62% when compared to BNNC [40] under various simulation conditions. This improvement in throughput is a result of the utilization of temporal throughput levels in GA, which facilitates the selection of throughput-aware routing paths. This makes the model useful for applications with a high data rate.

On the basis of PDR estimation, it can be seen that the proposed model is capable of improving the PDR achieved during communication by 8.35% compared to LEMH [2], 8.80% compared to MGA [19], and 7.70% compared to BNNC [40] under various simulation conditions. This improvement in PDR is due to the utilization of temporal PDR levels in GA, which aids in the selection of PDR-aware routing paths. This makes the model applicable for applications with a high data dissemination rate. On the basis of these jitter estimations, it can be seen that the proposed model is capable of reducing communication jitter by 6.08% when compared to LEMH [2], 20.23% when compared to MGA [19], and 27.58% when compared to BNNC [40] under various simulation conditions. This reduction is due to the utilization of temporal delay and throughput levels in GA, which facilitates the selection of low-jitter routing paths. This makes the model applicable to applications that require a high level of data consistency during communications. Due to these optimizations, the proposed model is useful for a wide range of real-time deployments that require low delay, low energy consumption, high throughput, high PDR, and low communication jitter.

In the future, the performance of the proposed model must be evaluated on larger network scenarios, and can be enhanced through the application of transformer-based optimizers such as Generative Adversarial Networks (GANs), Auto Encoders (AEs), etc. This performance can also be improved by employing low-complexity linear optimization techniques that employ regressive models for traffic pre-emption in real-time use cases.

V. References

[1] M. Besta et al., "High-Performance Routing With Multipathing and Path Diversity in Ethernet and HPC Networks," in IEEE Transactions on Parallel and Distributed Systems, vol. 32, no. 4, pp. 943-959, 1 April 2021, https://doi.org/10.1109/TPDS.2020.3035761

[2] Z. Wang, L. Shao, S. Yang and J. Wang, "LEMH: Low-Energy-First Electoral Multipath Alternating Multihop Routing Algorithm for Wireless Sensor Networks," in IEEE Sensors Journal, vol. 22, no. 16, pp. 16687-16704, 15 Aug.15, 2022, https://doi.org/10.1109/JSEN.2022.3191321.

[3] N. Maksić, "Topology Independent Multipath Routing for Data Center Networks," in IEEE Access, vol. 9, pp. 128590-128600, 2021, https://doi.org/10.1109/ACCESS.2021.3107236

[4] X. Fu, Y. Yang and O. Postolache, "Sustainable Multipath Routing Protocol for Multi-Sink Wireless Sensor Networks in Harsh Environments," in IEEE Transactions on Sustainable Computing, vol. 6, no. 1, pp. 168-181, 1 Jan.-March 2021, https://doi.org/10.1109/TSUSC.2020.2976096

[5] T. Zhu, X. Chen, L. Chen, W. Wang and G. Wei, "GCLR: GNN-Based Cross Layer Optimization for Multipath TCP by Routing," in IEEE Access, vol. 8, pp. 17060-17070, 2020, https://doi.org/10.1109/ACCESS.2020.2966045

[6] J. Zhang, "Online Multipath Routing via Multiplicative Weight Update," in IEEE Systems Journal, vol. 16, no. 3, pp. 3829-3832, Sept. 2022, https://doi.org/10.1109/JSYST.2021.3114393

[7] F. Jiang, Q. Zhang, Z. Yang and P. Yuan, "A Space–Time Graph Based Multipath Routing in Disruption-Tolerant Earth-Observing Satellite Networks," in IEEE Transactions on Aerospace and Electronic Systems, vol. 55, no. 5, pp. 2592-2603, Oct. 2019, https://doi.org/10.1109/TAES.2019.2938447

[8] Z. Chen, W. Zhou, S. Wu and L. Cheng, "An Adaptive on-Demand Multipath Routing Protocol With QoS Support for High-Speed MANET," in IEEE Access, vol. 8, pp. 44760-44773, 2020, https://doi.org/10.1109/ACCESS.2020.2978582

[9] P. Amaral, P. Pinto and L. Bernardo, "Achieving Correct Hop-by-Hop Forwarding on Multiple Policy-Based Routing Paths," in IEEE Transactions on Network Science and Engineering, vol. 7, no. 3, pp. 1226-1238, 1 July-Sept. 2020, https://doi.org/10.1109/TNSE.2019.2915515

[10] F. Tang, H. Zhang and L. T. Yang, "Multipath Cooperative Routing with Efficient Acknowledgement for LEO Satellite Networks," in IEEE Transactions on Mobile Computing, vol. 18, no. 1, pp. 179-192, 1 Jan. 2019, https://doi.org/10.1109/TMC.2018.2831679

[11] H. Geng et al., "A hybrid link protection scheme for ensuring network service availability in link-state routing networks," in Journal of Communications and Networks, vol. 22, no. 1, pp. 46-60, Feb. 2020, https://doi.org/10.1109/JCN.2019.000056

[12] J. Li, V. Giotsas, Y. Wang and S. Zhou, "BGP-Multipath Routing in the Internet," in IEEE Transactions on Network and Service Management, vol. 19, no. 3, pp. 2812-2826, Sept. 2022, https://doi.org/10.1109/TNSM.2022.3177471

[13] R. K. Lenka, A. K. Rath and S. Sharma, "Building Reliable Routing Infrastructure for Green IoT Network," in IEEE Access, vol. 7, pp. 129892-129909, 2019, https://doi.org/10.1109/ACCESS.2019.2939883

[14] G. Han, H. Wang, X. Miao, L. Liu, J. Jiang and Y. Peng, "A Dynamic Multipath Scheme for Protecting Source-Location Privacy Using Multiple Sinks in WSNs Intended for IIoT," in IEEE Transactions on Industrial Informatics, vol. 16, no. 8, pp. 5527-5538, Aug. 2020, https://doi.org/10.1109/TII.2019.2953937

[15] S. M. Shimly, D. B. Smith and S. Movassaghi, "Experimental Analysis of Cross-Layer Optimization for Distributed Wireless Body-to-Body Networks," in IEEE Sensors Journal, vol. 19, no. 24, pp. 12494-12509, 15 Dec.15, 2019, https://doi.org/10.1109/JSEN.2019.2937356

[16] J. Rischke, P. Sossalla, H. Salah, F. H. P. Fitzek and M. Reisslein, "QR-SDN: Towards Reinforcement Learning States, Actions, and Rewards for Direct Flow Routing in Software-Defined Networks," in IEEE Access, vol. 8, pp. 174773-174791, 2020, https://doi.org/10.1109/ACCESS.2020.3025432

[17] R. Zhu et al., "Survival Multipath Energy-Aware Resource Allocation in SDM-EONs During Fluctuating Traffic," in Journal of Lightwave Technology, vol. 39, no. 7, pp. 1900-1912, 1 April1, 2021, https://doi.org/10.1109/JLT.2020.3043271

[18] H. Yao, H. Liu, P. Zhang, S. Wu, C. Jiang and S. Guo, "A Learning-Based Approach to Intra-Domain QoS Routing," in IEEE Transactions on Vehicular Technology, vol. 69, no. 6, pp. 6718-6730, June 2020, https://doi.org/10.1109/TVT.2020.2986769

[19] A. Bhardwaj and H. El-Ocla, "Multipath Routing Protocol Using Genetic Algorithm in Mobile Ad Hoc Networks," in IEEE Access, vol. 8, pp. 177534-177548, 2020, https://doi.org/10.1109/ACCESS.2020.3027043

[20] J. Alvarez-Horcajo, D. Lopez-Pajares, I. Martinez-Yelmo, J. A. Carral and J. M. Arco, "Improving Multipath Routing of TCP Flows by Network Exploration," in IEEE Access, vol. 7, pp. 13608-13621, 2019, https://doi.org/10.1109/ACCESS.2019.2893412

[21] T. Zhang, S. Zhao and B. Cheng, "Multipath Routing and MPTCP-Based Data Delivery Over Manets," in IEEE Access, vol. 8, pp. 32652-32673, 2020, https://doi.org/10.1109/ACCESS.2020.2974191

[22] C. -M. Yu, M. -L. Ku and L. -C. Wang, "BMRHTA: Balanced Multipath Routing and Hybrid Transmission Approach for Lifecycle Maximization in WSNs," in IEEE Internet of Things Journal, vol. 9, no. 1, pp. 728-742, 1 Jan.1, 2022, https://doi.org/10.1109/JIOT.2021.3085597

[23] W. Zhang, W. Lei and S. Zhang, "A Multipath Transport Scheme for Real-Time Multimedia Services Based on Software-Defined Networking and Segment Routing," in IEEE Access, vol. 8, pp. 93962-93977, 2020, https://doi.org/10.1109/ACCESS.2020.2994346

[24] Y. H. Robinson et al., "Link-Disjoint Multipath Routing for Network Traffic Overload Handling in Mobile Ad-hoc Networks," in IEEE Access, vol. 7, pp. 143312-143323, 2019, https://doi.org/10.1109/ACCESS.2019.2943145

[25] U. Srilakshmi, N. Veeraiah, Y. Alotaibi, S. A. Alghamdi, O. I. Khalaf and B. V. Subbayamma, "An Improved Hybrid Secure Multipath Routing Protocol for MANET," in IEEE Access, vol. 9, pp. 163043-163053, 2021, https://doi.org/10.1109/ACCESS.2021.3133882

[26] Y. Huang, X. Jiang, S. Chen, F. Yang and J. Yang, "Pheromone Incentivized Intelligent Multipath Traffic Scheduling Approach for LEO Satellite Networks," in IEEE Transactions on Wireless Communications, vol. 21, no. 8, pp. 5889-5902, Aug. 2022, https://doi.org/10.1109/TWC.2022.3144189

[27] K. Sakai, M. -T. Sun, W. -S. Ku, J. Wu and T. H. Lai, "Secure Data Communications in Wireless Networks Using Multi-Path Avoidance Routing," in IEEE Transactions on Wireless Communications, vol. 18, no. 10, pp. 4753-4767, Oct. 2019, https://doi.org/10.1109/TWC.2019.2928801

[28] Y. Zhang, X. An, M. Yuan, X. Bu and J. An, "Concurrent Multipath Routing Optimization in Named Data Networks," in IEEE Internet of Things Journal, vol. 7, no. 2, pp. 1451-1463, Feb. 2020, https://doi.org/10.1109/JIOT.2019.2955139

[29] L. Qu, C. Assi, M. J. Khabbaz and Y. Ye, "Reliability-Aware Service Function Chaining With Function Decomposition and Multipath Routing," in IEEE Transactions on Network and Service Management, vol. 17, no. 2, pp. 835-848, June 2020, https://doi.org/10.1109/TNSM.2019.2961153

[30] S. Devaraju, M. Parsinia, E. S. Bentley and S. Kumar, "A Multipath Local Route Repair Scheme for Bidirectional Traffic in an Airborne Network of Multibeam FDD Nodes," in IEEE Transactions on Aerospace and Electronic Systems, vol. 58, no. 4, pp. 2983-2995, Aug. 2022, https://doi.org/10.1109/TAES.2022.3145298

[31] L. Chen, B. Hu, Z. -H. Guan, L. Zhao and X. Shen, "Multiagent Meta-Reinforcement Learning for Adaptive Multipath Routing Optimization," in IEEE Transactions on Neural Networks and Learning Systems, vol. 33, no. 10, pp. 5374-5386, Oct. 2022, http://doi.org/10.1109/TNNLS.2021.3070584

[32] F. H. Kumbhar and S. Y. Shin, "VAR²: Novel Vehicular Ad-Hoc Reliable Routing Approach for Compatible and Trustworthy Paradigm," in IEEE Communications Letters, vol. 25, no. 2, pp. 670-674, Feb. 2021, https://doi.org/10.1109/LCOMM.2020.3032753

[33] H. Bi, Y. Chen and X. Zhu, "A Multipath Routing for Payment Channel Networks for Internet of Things Microtransactions," in IEEE Internet of Things Journal, vol. 9, no. 20, pp. 19670-19681, 15 Oct.15, 2022, https://doi.org/10.1109/JIOT.2022.3167098

[34] M. Park, S. Sohn, K. Kwon and T. T. Kwon, "MaxPass: Credit-based multipath transmission for load balancing in data centers," in Journal of Communications and Networks, vol. 21, no. 6, pp. 558-568, Dec. 2019, https://doi/org/10.1109/JCN.2019.000047

[35] M. Karaata, A. Al-Mutairi and S. Alsubaihi, "Multipath Routing Over Star Overlays for Quality of Service Enhancement in Hybrid Content Distribution Peer-to-Peer Networks," in IEEE Access, vol. 10, pp. 7042-7058, 2022, https://doi.org/10.1109/ACCESS.2021.3139936

[36] A. Abugabah, A. A. Alzubi, O. Alfarraj, M. Al-Maitah and W. S. Alnumay, "Intelligent Traffic Engineering in Software-Defined Vehicular Networking Based on Multi-Path Routing," in IEEE Access, vol. 8, pp. 62334-62342, 2020, https://doi.org/10.1109/ACCESS.2020.2983204

[37] J. Tapolcai, G. Rétvári, P. Babarczi and E. R. Bérczi-Kovács, "Scalable and Efficient Multipath Routing via Redundant Trees," in IEEE Journal on Selected Areas in Communications, vol. 37, no. 5, pp. 982-996, May 2019, https://doi.org/10.1109/JSAC.2019.2906742

[38] C. Han, J. Yin, L. Ye and Y. Yang, "NCAnt: A Network Coding-Based Multipath Data Transmission Scheme for Multi-UAV Formation Flying Networks," in IEEE Communications Letters, vol. 25, no. 3, pp. 1041-1044, March 2021, https://doi.org/10.1109/LCOMM.2020.3039846

[39] V. Di Valerio, F. Lo Presti, C. Petrioli, L. Picari, D. Spaccini and S. Basagni, "CARMA: Channel-Aware Reinforcement Learning-Based Multi-Path Adaptive Routing for Underwater Wireless Sensor Networks," in IEEE Journal on Selected Areas in Communications, vol. 37, no. 11, pp. 2634-2647, Nov. 2019, https://doi.org/10.1109/JSAC.2019.2933968

[40] Y. Zhang, P. Dong, X. Du, H. Luo, T. Zheng and M. Guizani, "BNNC: Improving Performance of Multipath Transmission in Heterogeneous Vehicular Networks," in IEEE Access, vol. 7, pp. 158113-158125, 2019, https://doi.org/10.1109/ACCESS.2019.2948954

[41] W. Mei and R. Zhang, "Intelligent Reflecting Surface for Multi-Path Beam Routing With Active/Passive Beam Splitting and Combining," in IEEE Communications Letters, vol. 26, no. 5, pp. 1165-1169, May 2022, https://doi.org/10.1109/LCOMM.2022.3152320